Minerals Engineering 196 (2023) 108050

Contents lists available at ScienceDirect

Minerals Engineering

journal homepage: www.elsevier.com/locate/mineng

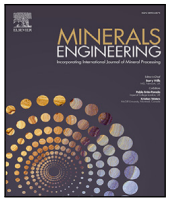

Economic model predictive control for a rougher froth flotation cell using physics-based models

Paulina Quintanilla [a,*], Daniel Navia [b], Stephen J. Neethling [a], Pablo R. Brito-Parada [a]

[a] Department of Earth Science and Engineering, Royal School of Mines, Imperial College London, South Kensington Campus, United Kingdom
[b] Departamento de Ingeniería Química y Ambiental, Universidad Técnica Federico Santa María, Campus San Joaquín, Santiago, Chile

ARTICLE INFO

Keywords:
Economic model predictive control
Froth flotation
Froth flotation control
Mineral processing
Orthogonal collocations
Sensitivity analysis

ABSTRACT

The development of an economic model predictive control (E-MPC) strategy is presented. The strategy uses a novel dynamic flotation model that incorporates the physics of the froth phase in a flotation cell. The dynamic model was previously calibrated and validated using experimental data.

Sensitivity analyses were conducted to select a suitable objective function that accounted for both process economics and control variable sensitivities. While the ultimate goal of a rougher flotation cell is to maximise the metallurgical recovery at a steady state for a specified minimum grade, it was evident that the incorporation of air recovery dynamics (which can be measured in real-time) and concentrate grade dynamics (calculated through first-principle models) led to the best results. The addition of a dynamic variable that can be easily measured online, i.e. air recovery, offers great potential to improve plant performance in existing froth flotation systems. Furthermore, a minimum concentrate grade was imposed in the E-MPC strategy. This acts as an economic constraint as it allows the metallurgical recovery to be optimised while ensuring that concentrate grade requirements are met.

The dynamic optimisation problem for the E-MPC strategy was discretised using orthogonal collocations, and was implemented in Matlab using automatic differentiation via CasADi. Two typical manipulated variables were considered: air flowrate and pulp height setpoints. Based on laboratory-scale data, the implementation of the E-MPC strategy resulted in improvements ranging from +8 to +22 % in metallurgical recovery, while maintaining the specified grade. This is therefore an encouraging control strategy to explore in larger flotation systems.

1. Introduction

Much recent research has focused on advanced control and optimisation techniques to improve plant performance. Model predictive control (MPC) is widely recognised as one of the most efficient advanced control techniques to improve the performance of a process (Mahmoodi et al., 2009). However, in comparison to other chemical industries, the mineral processing sector still lacks successful implementation of such advanced techniques (Pérez-García et al., 2021). Particularly for froth flotation, the potential of implementing MPC strategies has remained untapped this far because of the difficulties in modelling this process due to its complex dynamics.

Most models for froth flotation control are oversimplified, in particular neglecting the phenomena within the froth phase. The importance of modelling the froth lies in the fact that the phenomena occurring there ultimately determine the separation efficiency and thus have a significant impact on the metallurgical recovery and, especially, the concentrate grade. For a critical review on modelling for flotation control, the reader is referred to Quintanilla et al. (2021a).

In terms of MPC implementation for flotation control, Maldonado et al. (2007) proposed an optimal control for a rougher flotation circuit using dynamic programming. They suggested a control strategy for the first three flotation banks for regulation while maintaining deep froth depths in the last two flotation banks. Their results were validated against industrial data, showing good agreement with the actual operational performance. The authors were concerned about the high computational load of the proposed optimisation strategy. However, in the intervening fifteen years, there has been a significant increase in the available computational resources allowing for the

* Correspondence to: Sargent Centre for Process Systems Engineering, Department of Chemical Engineering, Imperial College London, South Kensington Campus, United Kingdom.
E-mail address: p.quintanilla@imperial.ac.uk (P. Quintanilla).

https://doi.org/10.1016/j.mineng.2023.108050
Received 7 January 2023; Received in revised form 1 March 2023; Accepted 6 March 2023
Available online 11 March 2023

solution of complex optimisation problems (e.g. large-scale, nonlinear, non-convex, among others) (Ellis et al., 2014). In Maldonado et al. (2009), a Proportional–Integral (PI) controller was combined with a constrained MPC strategy to optimise a two-phase (gas-water) pilot flotation column. The controlled variables were froth depth, gas holdup and bias rate, while the manipulated variables were tailings, wash-water and air flowrates. The MPC strategy was formulated to track the error in the gas holdup and bias rate under certain operating constraints. The same two-phase pilot flotation column was subsequently used by Riquelme et al. (2016) to develop a predictive control of the bubble size distribution (BSD). BSD is an important factor in froth flotation since it is related to the surface area available for particle attachment due to differences in surface properties (Mesa et al., 2022). A Wiener model was used to estimate and control the BSD. A Wiener model consists of a linear system followed by a unitary gain in series with a static non-linear element (Billings and Fakhouri, 1977). It is a suitable option for multiple-input multiple-output (MIMO) systems in which multiple linear variables are dependent upon a nonlinear element (Riquelme et al., 2015). Riquelme et al. (2016), however, did not link the influence of the BSD to flotation performance indicators, such as concentrate grade and metallurgical recovery.

To date, few studies have reported MPC implementation at the industrial scale in the flotation process; yet, all of these studies have used empirical models. For example, Brooks and Koorts (2017) proposed a model predictive control strategy for a zinc flotation circuit using online X-ray fluorescence analysers, based on empirical dynamic models from plant step test data. As a result, significant reductions in reagents were achieved while maintaining grade constraints. However, the main challenges were related to the slow measurement frequency of the X-ray fluorescence analysers, as well as the necessity of validating the sensor for the measurements. The authors also remarked that dealing with control room operators and some metallurgists and engineers on site was not an easy task. It seems natural for operators to challenge any new idea that contradicts their own established control strategies, which may have worked well for them for years. In Brooks and Munalula (2017), cascaded model predictive controllers were implemented at the industrial scale. The controlled variables were froth velocity and X-ray fluorescence analysers, and the manipulated variables were air flowrate, pulp height, and frother dosage setpoints. Empirical models based on Finite Impulse Responses (FIR) were developed and implemented in the MPC strategy. Although encouraging results were obtained from this MPC implementation, the authors also identified challenges related to measurement validation. They proposed a scheme based on high/low limits, but this has the disadvantage that there are several tuning and sensing decisions that are based on experience rather than formal analysis.

With regard to economic optimisation in froth flotation, steady-state models are generally implemented via real-time optimisation (RTO) strategies, such as those found in Sbarbaro et al. (2008) and Navia et al. (2019). Nonetheless, although steady-state operations are typical in chemical process industries, they may not be the best economic strategy given the dynamic nature of many of these systems (Ellis et al., 2014). The integration of economics into the process control layer (dynamic) is known as economic model predictive control (E-MPC) (Diehl et al., 2011; Amrit et al., 2011; Huang et al., 2011; Liu et al., 2015; Schäfer et al., 2019). E-MPC considers both closed-loop stability and dynamic performance (Ellis et al., 2014). It is important to point out that the term "economic" does not necessarily imply that the objective function is in currency terms but rather can be a reflection of the economics of the process. This is further discussed in Ellis et al. (2014), where an example of E-MPC implementation to maximise production in a reactor using kinetic models is given.

The main contribution of this paper is therefore to present the first E-MPC strategy developed for the froth flotation process. A novel phenomenological dynamic model that includes the froth physics was used in this study, which was developed by Quintanilla et al. (2021c), and calibrated and validated using experimental data, as shown in Quintanilla et al. (2021b). An optimal objective function was proposed to maximise the metallurgical recovery while ensuring a minimum limit on the concentrate grade. The objective function was built based on available online measurements and process economics and was supported by thorough sensitivity analyses with respect to the degrees of freedom, i.e. air flowrate and pulp height setpoints. It was established that the incorporation of the dynamic evolution of air recovery (measured online) and the concentrate grade (estimated using first-principle models) into the objective function would lead to optimal results.

The nomenclature and the relevant background theory are presented in Section 2. An overview of the dynamic model, modifications and assumptions are shown in Section 3. Sensitivity analyses of the different terms in the objective function are presented in Section 4. The optimal control problem formulation is presented in Section 5, whereas simulation results of the economic model predictive control strategy are discussed in Section 6.

2. Preliminaries

2.1. Nomenclature

The notation used in this work is standard. Bold lowercase symbols represent column vectors. $\mathbf{x}(t) \in \mathbb{R}^{N_x}$ is a vector of state variables, $\mathbf{y}(t) \in \mathbb{R}^{N_y}$ is a vector of process variables, $\mathbf{u}(t) \in \mathbb{R}^{N_u}$ is a vector of control inputs, and $\mathbf{z}(t) \in \mathbb{R}^{N_z}$ is a vector of algebraic variables, $\boldsymbol{\beta}$ is a vector of parameters of an objective function, $\mathbf{p}$ is a vector of parameters of the model, and t_f is the final time. Each discrete time is represented by t_n. The prediction horizon is N_p and the control horizon is N_c.

For the dynamic model of the process, $\tilde{\bullet}$ refers to normalised variables (states and time). Nomenclature of all variables of the model of the process, including further explanation of each variable can be found in Quintanilla et al. (2021c,b).

2.2. Economic optimisation and process control

Generally, economic optimisation and process control are carried out in different layers, as shown in Fig. 1. The upper layer is known as the real-time optimisation (RTO) layer, in which the economic optimisation is performed based on steady-state models of the process (Liu et al., 2015). The RTO layer gives instructions to a lower layer, which corresponds to the supervisory control (Liu et al., 2005; Engell, 2007; Navia et al., 2018).

In the supervisory layer, MPC can be used as an advanced control strategy due to its ability to handle multivariate processes, taking into consideration process constraints. A schematic of the MPC strategy is shown in Fig. 2. MPC relies upon a dynamic model of the process to predict the future behaviour of important variables (Qin and Badgwell, 1997; Camacho and Bordons, 2007). Specifically, the model is used to solve a dynamic optimisation problem while taking into account process constraints in order to obtain a control action sequence for the manipulated variables (Camacho and Bordons, 2007; Sbarbaro and del Villar, 2010; Bergh and Yianatos, 2011; Ellis et al., 2014). Process constraints and multivariable interactions can be also added to the optimisation problem, which allows the implementation of MPC into multiple-input, multiple-output (MIMO) nonlinear systems.

Standard MPC for supervisory control uses a quadratic performance index, which corresponds to measurements of the predicted deviation of the error of process variables ($\mathbf{y} - \mathbf{y}^{\mathbf{sp}}$), where $\mathbf{y}$ is the process variable and $\mathbf{y}^{\mathbf{sp}}$ is the setpoint, and inputs ($\mathbf{u}$) from their corresponding

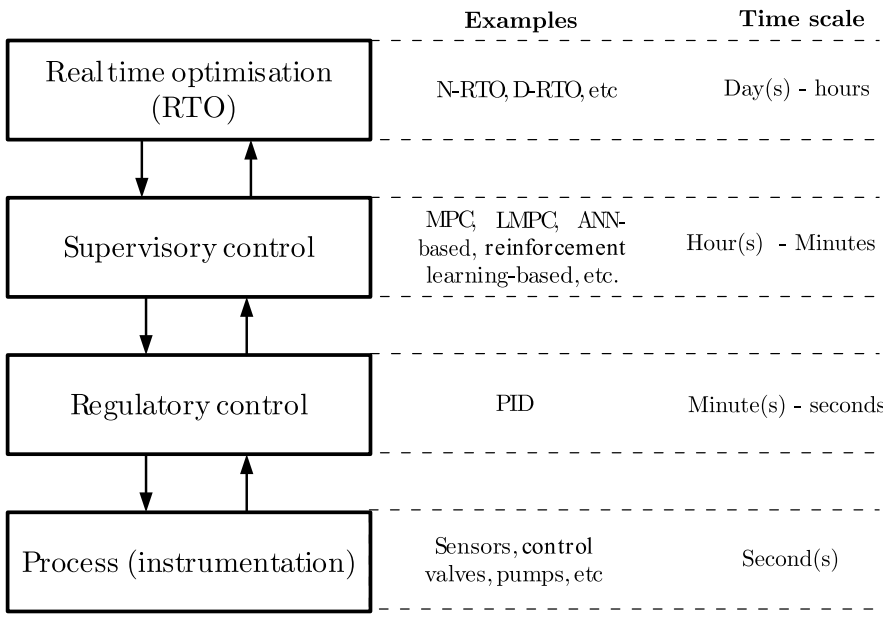

Fig. 1. Classic control hierarchy for process optimisation and control. Adapted from Rawlings et al. (2013) and Ellis et al. (2014).

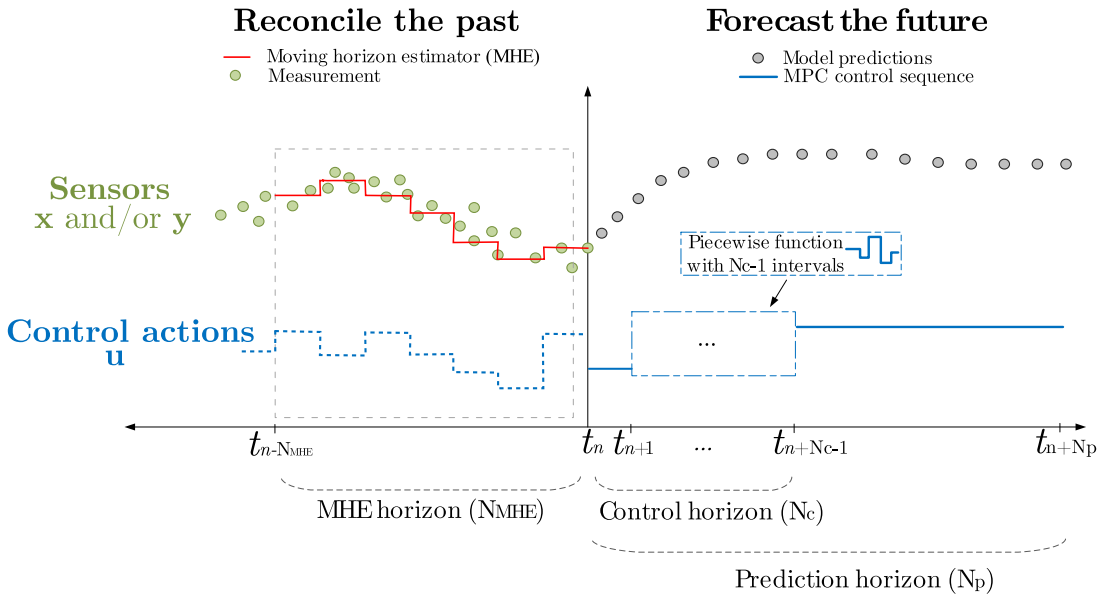

Fig. 2. Schematic of the model predictive control strategy. A dynamic model of the process is used to forecast the future (grey dots). At the same time, the MPC strategy gives the best control sequence **u** (blue piecewise curve) to maximise or minimise the objective function. Green dots are the measurements from the sensors (**x**: states, and/or **y**: process variables), which allow for the estimation of new states (red curve) every time that the prediction and control horizons are shifted. (For interpretation of the references to colour in this figure legend, the reader is referred to the web version of this article.)

steady-state values, to force the process to the nominal steady-state. The classic dynamic optimisation problem is shown in Eqs. (1a)–(1e):

$$\underset{\mathbf{u}\in\mathbb{R}^{N_u}}{\text{minimise}} \int_0^{t_{N_p}} \left(\|\mathbf{y}(t) - \mathbf{y}^{\mathbf{SP}}\|^2_{\boldsymbol{\beta}_1} + \|\Delta\mathbf{u}(t)\|^2_{\boldsymbol{\beta}_2} \right) dt, \tag{1a}$$

subject to

$$\frac{d\mathbf{x}}{dt} = f_{MPC}(\mathbf{x}(t), \mathbf{u}(t), \mathbf{p}) \quad \forall t \in \left[t_n, t_{N_p}\right], \tag{1b}$$

$$\mathbf{x}(0) = \mathbf{x}\left(t_n\right), \tag{1c}$$

$$g(\mathbf{x}(t), \mathbf{u}(t)) \leq 0, \quad \forall t \in \left[t_n, t_{N_p}\right), \tag{1d}$$

$$\mathbf{y}(t) = \mathbf{h}(\mathbf{x}(t), \mathbf{u}(t), \mathbf{p}), \tag{1e}$$

where β_1 and β_2 are tuning parameters that ensure a good trade-off between the speed of response in **y** and the cost of control action **u**. Eq. (1b) represents the predicted evolution of the states using a dynamic model. Initial conditions of the dynamic model (Eq. (1c)) are obtained at each sampling period thanks to the measurements of current process variables/states. Note that it is not always possible to have measurements of all states and, therefore, an estimator strategy such as a moving horizon estimator (MHE) should be implemented. The process constraints are also considered (Eq. (1d)) in the optimisation. Eq. (1e) denotes the model equations for the process variables **y**,

which can be calculated from the model of the process and/or can be measured online.

MPC is implemented following a receding horizon strategy, which means that only the first step of the control sequence is applied to the real system. That is to say, the first control action is sent to the control actuators to be implemented over the sampling period, i.e. from t_n to t_{n+1}. After an appropriate time, the horizon is shifted one Δt. At the next sampling period, the MPC (Eq. (1a) to (1e)) is resolved, and the new first step of the control sequence is applied to the real system.

One of the disadvantages of hierarchical control (Fig. 1) is that it neglects the economic performance of the dynamic process (Liu and Cui, 2018). A promising alternative for optimisation is to implement RTO and MPC in a single layer to enable dynamic process optimisation has been attracting widespread attention (Ellis et al., 2014). This is known as economic model predictive control (E-MPC). There is extensive literature on the theoretical framework for E-MPC concerning stability and optimality properties (see Diehl et al. (2011), Angeli et al. (2012), Heidarinejad et al. (2012), Ellis et al. (2014), Liu et al. (2015)). The use of E-MPC has some requirements that need to be met. For example, the dynamic optimisation must be carried out on time scales that are sufficient for both economic performance evaluation and disturbance rejection (Schäfer et al., 2019). The standard formulation of the quadratic cost in Eq. (1a) allows a closed-loop response to be obtained. Nevertheless, it may not be appropriate for dynamic economic optimisation (E-MPC). A general form of the E-MPC problem is given below:

$$\underset{\mathbf{u}\in\mathbb{R}^{N_u}}{\text{minimise}} \int_{t_n}^{t_{N_p}} l_e(\mathbf{x}(t),\mathbf{u}(t))dt, \tag{2a}$$

subject to

$$\frac{d\mathbf{x}}{dt} = f_{EMPC}(\mathbf{x}(t),\mathbf{u}(t),p) \quad \forall t \in \left[t_n, t_{N_p}\right), \tag{2b}$$

$$\mathbf{x}(0) = \mathbf{x}\left(t_n\right), \tag{2c}$$

$$g(\mathbf{x}(t),\mathbf{u}(t)) \le 0, \quad \forall t \in \left[t_n, t_{N_p}\right). \tag{2d}$$

The E-MPC strategy is also implemented in a receding horizon fashion. The objective function in Eq. (2a) is different from the one presented in Eq. (1a) as the economic cost function is considered through the dynamic operation of the process (Ellis et al., 2014). Furthermore, a linear model of the process (f_{MPC} in Eq. (1b)) is usually sufficient for standard MPC because of its regulatory control purpose. However, although linear models are relatively easy to solve, they lose generality as they are accurate only in a narrow operating condition range. In contrast, the economic objective of an E-MPC needs a more general model of the process (f_{EMPC} in Eq. (2b)) that allows optimal operating conditions to be found over a wider range. This means that phenomenological, nonlinear models are usually the best option for E-MPC implementation. However, due to the challenges in solving this type of model, an E-MPC implementation is not always widely explored. Our study, therefore, provides the first E-MPC implementation in a froth flotation cell using a phenomenological dynamic model.

2.3. Direct methods for optimal control problems

In order to implement an MPC or E-MPC strategy, it is necessary to solve in a closed-loop an optimal control problem (OCP), repeatedly, accounting for the feedback from each loop. The OCP is the dynamic optimisation problem presented in Eqs. (1a)–(1d) (MPC) and Eqs. (2a)–(2d) (E-MPC), which is solved in a receding fashion. Direct methods to convert the infinite-dimensional OCP to a finite-dimensional nonlinear programming problem (NLP) have been extensively studied for over 40 years (e.g. Tsang et al., 1975; Cuthrell and Biegler, 1987; Fabien, 1998; Chachuat et al., 2006; Biegler, 2007, 2010). Direct methods involve discretising the optimisation problem and applying NLP techniques to the resulting finite-dimensional optimisation problem. The discretisation approaches can be divided into two sub-categories: sequential and simultaneous (Chachuat et al., 2006). Flowcharts of both sequential and simultaneous methods are presented in Fig. 3.

As can be seen from Fig. 3, in the sequential methods, only the control variables are discretised, and a DAE (differential and algebraic equations) solver is embedded in the NLP problem. While the sequential methods are relatively easy to implement (Beck, 2010), they usually fail for unstable and ill-conditioned systems (Biegler, 2010). In contrast to the sequential methods, simultaneous methods do not use a computationally expensive embedded DAE solver. Instead, both state and control variables are discretised using collocations over finite intervals in time, as a Runge–Kutta method, and are approximated as polynomials over each finite interval. The best-known approach for simultaneous methods is called orthogonal collocations across finite elements (Fig. 4). The differential equations are discretised at selected interpolation points ($\tau_{n_j}, j = 1,\ldots,3$ in Fig. 4) across every sampling time. Once the interpolation points are defined, polynomial approximations of the state $\mathbf{x}(t)$, and piecewise polynomials of the control $\mathbf{u}(t)$, are considered. These polynomial approximations, also known as collocation equations, are algebraic equations that are easy to derive and are therefore incorporated directly within the NLP implementation. Details on the theorems and a full derivation of collocation equations can be found in Biegler (2010).

While all three discretisation methods were implemented in this study, the sequential methods were found to be impractical. Specifically, sequential methods had an elapsed time of over 150 s for each loop, while orthogonal collocations solved the dynamic optimisation in less the one second (generally as low as 600 ms). The large differences in resolution times are due to the fact that convergence is improved in simultaneous methods by avoiding an embedded solver, and sensitivity calculations from the solver are replaced by direct gradient and Hessian evaluations within the NLP implementation taking advantage of the sparsity of the corresponding matrices (Biegler, 2010). Therefore, in this study, only the results using orthogonal collocations and automatic differentiation, are discussed in Section 6.

2.4. CasADi framework for nonlinear programming problems (NLP)

The dynamic optimisation problem in this study was implemented in Matlab R2020B using CasADi (Andersson et al., 2019). CasADi is an open-source software tool that allows large-scale optimisation for DAE systems to be solved. CasADi uses a symbolic framework to efficiently obtain the derivatives of the problem using automatic differentiation. It has embedded integrators for ODE and DAE systems. Embedded NLP solvers, such as interior point methods and sequential quadratic programming are also included. It also allows dynamic systems with algebraic loops to be solved via an embedded root-finding solver.

In this study, the three direct discretisation methods (i.e. single shooting, multiple shooting and orthogonal collocations) were implemented using CasADi. As shown in Fig. 3, the sequential methods require an integrator for the DAE system. In both sequential cases, an IDAS integrator was used. The IDAS integrator is described in Serban et al. (2021). The NLP solver was the *Interior Point Optimizer* (IPOPT), which is described in Curtis et al. (2012).

3. Dynamic froth flotation model overview

The dynamic model developed by Quintanilla et al. (2021c) was used to make predictions for the E-MPC. The model was calibrated and validated with experimental data from Quintanilla et al. (2021b). An overview of the main aspects of the dynamic model and considerations are presented in this section. Nevertheless, for a comprehensive understanding of the model development and the physical meaning of all the variables, the reader is referred to Quintanilla et al. (2021c,b).

The E-MPC strategy proposed in this study considers a rougher froth flotation cell. The rougher cell objective is to recover as much valuable

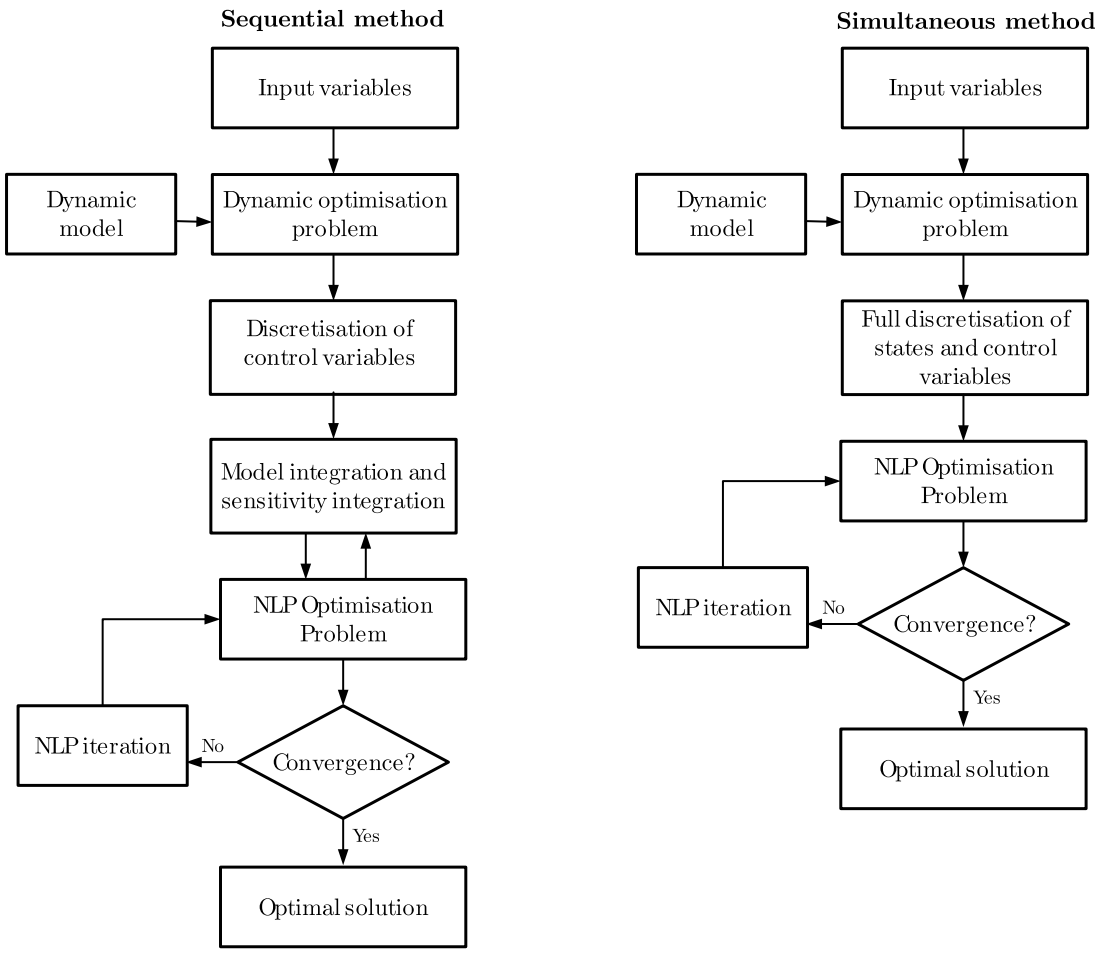

Fig. 3. Flowchart of the direct optimisation methods. Left: sequential method (e.g. single shooting and multiple shooting). Right: simultaneous method (e.g. orthogonal collocations). *Source:* Adapted from Rohman and Aziz (2019).

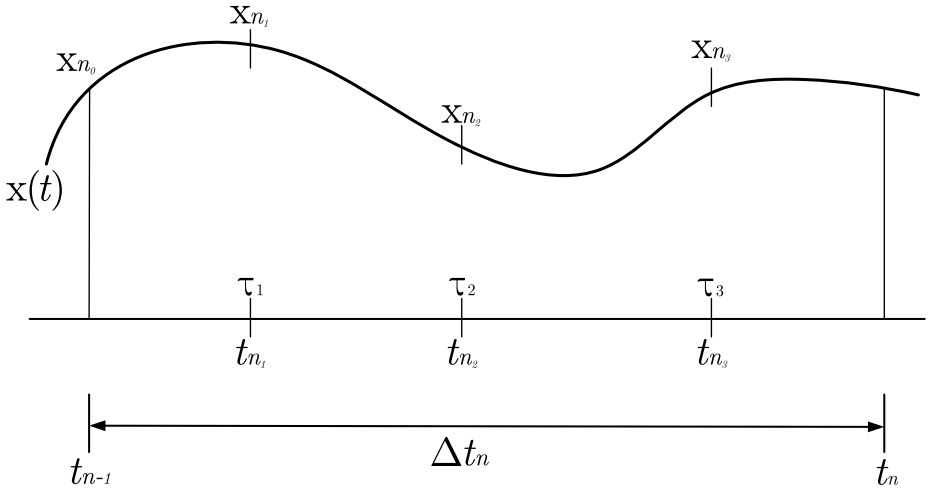

Fig. 4. Polynomial approximation for state profile, $\mathbf{x}(t)$, across a finite element, Δt, in the orthogonal collocation strategy. *Source:* Adapted from Biegler (2010).

metal as possible while maintaining the desired concentrate grade. The concentrate is sent to further stages, usually to cleaning cells, where the objective is to increase the concentrate grade. A piping and instrument diagram (P&ID) of a typical rougher flotation cell is presented in Fig. 5, which consists of an air flowrate controller (FIC) and a pulp level controller (LIC). These are the manipulated variables in this study, as shown in Table 1, which are the most common manipulated variables in the vast majority of froth flotation plants.

The dynamic model is classified as a DAE system (i.e. composed of differential and algebraic equations), and it has a total of $26+5K+10I$

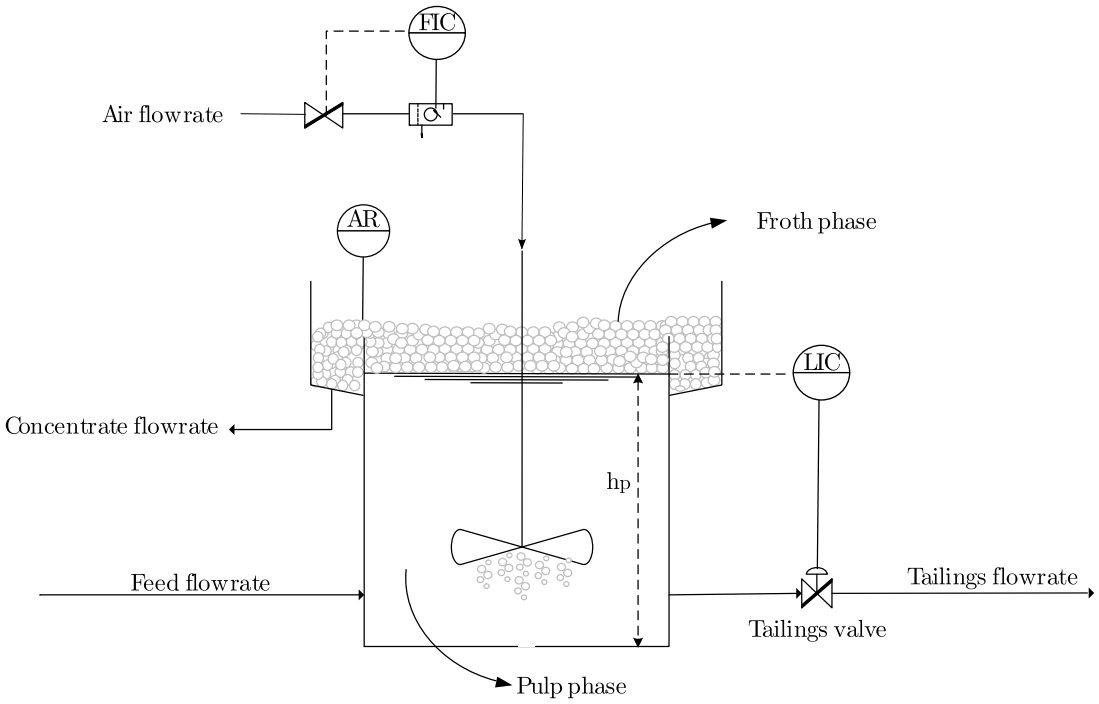

Fig. 5. P&ID of a typical froth flotation cell. FIC is a flowrate controller for the air flowrate, LIC is a level controller, and AR is an air recovery sensor. The AR sensor consists of two sensors: an optical laser, and one or more cameras (more information in Section 4). h_p refers to pulp height.

Table 1
Variables of the DAE system from Quintanilla et al. (2021c).

Variables	Nomenclature	Units
Control variables (u)		
Air flowrate setpoint	Q_{air}^{SP}	$m^3\ s^{-1}$
Pulp height setpoint	h_p^{SP}	m
States (x)		
Mass of mineralogical class $i = 1, \dots, I$	M_i	kg
Gas holdup of bubble size class $k = 1, \dots, K$	ϕ^k	–
Pulp height	h_p	m
Tailings flowrate	Q_{tails}	$m^3\ s^{-1}$
Algebraic variables (z)		
Air recovery	α	–
Froth air recovery	α^*	–

equations and $29 + 5K + 12I$ variables, where K is the number of bubble size classes, and I is the number of mineralogical classes used. The number of bubble size classes, K, allows better accuracy for the estimation of dynamic gas holdup (Shean et al., 2018). In this work, a total of 10 bubble size classes (i.e. $K = 10$) were considered, in addition to two mineralogical classes (i.e. $I = 2$): (1) Chalcopyrite as a valuable mineral, which contains 34.5% of copper, and (2) quartz as gangue. The values of the parameters a, b, and c of the bursting rate equation were the same as those found in Neethling and Brito-Parada (2018) assuming a quadratic relationship between bursting rate (v_b) and superficial air velocity (j_g). A quadratic relationship ensures that air recovery goes through a peak for a certain superficial air velocity (Hadler and Cilliers, 2009; Hadler et al., 2010; Neethling and Brito-Parada, 2018).

3.1. Model modifications and considerations

The original dynamic model was slightly modified to ease the control implementation. As can be seen from equations 41, 44, 54 and 57 in Quintanilla et al. (2021c), there are four variables defined with *if-else* statements: concentrate flowrate (Q_c), slurry content (ϵ), froth recovery (R_f), and entrainment factor (ENT). The *if-else* formulations define these variables depending on the value of air recovery (α) such that the model equations change when α is lower than or greater than 0.5. These model equations are continuous at $\alpha = 0.5$ and hence a sharp transition can be made.

The optimisation algorithm used in this study is derivative-based; however, derivatives for *if-else* formulations are not defined and therefore cannot be calculated. This issue was addressed by defining saturation (α^*_{sat}) and switch (S_F) functions that are differentiable. The saturation function was defined as a function of α^* (Equation 42 in Quintanilla et al. (2021c)) as follows:

$$\alpha^*_{sat}(\alpha^*) = a_{sat} + \frac{b_{sat}}{1 + \exp\left(-c_{sat}\left(\alpha^* - d_{sat}\right)\right)}, \tag{3}$$

where $a_{sat}, b_{sat}, c_{sat}, d_{sat}$ are tuning parameters. The switch function was defined as a sigmoid function as follows:

$$S_F(\alpha) = \frac{1}{1 - \exp\left(-a_{S_F}\left(\alpha - b_{S_F}\right)\right)}, \tag{4}$$

where a_{S_F}, and b_{S_F} are tuning parameters. Using Eqs. (3) and (4), a variable that is defined using *if-else* statements can be then approximated as a continuous, differentiable function (y) as follows:

$$y = (1 - S_F(\alpha))F_1(\alpha^*_{sat}) + S_F(\alpha)F_2(\alpha^*_{sat}), \tag{5}$$

where $F_1(\alpha^*_{sat})$ is the model equation for the variable if air recovery (α) is lower than 0.5, and $F_2(\alpha^*_{sat})$ if air recovery is greater or equal to 0.5. Note that $\alpha^*_{sat} \in (0, 1)$ and it replaces α^* in the original dynamic model to avoid numerical problems. The tuning parameters were calibrated, using a solver of nonlinear least-squares (*lsqnonlin*) in Matlab, for the four variables together to reduce the model complexity. The values for the tuning parameters are given in Table 2, assuming a_{S_F} and b_{S_F} equal to 50 and 0.5, respectively. A comparison of the results from the simulations using the original model (*if-else* statements) and sigmoid approximations (i.e. Eqs. (3)–(5)) are displayed in Fig. A.13 in Appendix A.

Additionally, a modified version of the model equation for gas holdup was used (Equation 17 in Quintanilla et al. (2021c)), where a

Table 2
Tuning parameters for Eq. (3).

Parameter	Value	95% confidence interval
a_{sat}	0.01	[0.001267, 0.01873]
b_{sat}	0.4927	[0.4764, 0.509]
c_{sat}	10.48	[9.312, 11.65]
d_{sat}	0.2588	[0.2464, 0.2712]

new variable was defined as: $\phi^k = \left(\frac{\epsilon_0^k}{1-\epsilon_{0,\ \text{total}}}\right)$. k refers to the bubble size class. Therefore, the ODE for gas holdup is now:

$$\frac{d\phi^k}{dt} = \frac{1+\phi^T}{A_{cell}h_p}\left(Q_{air}^k d_{b_{prop}}^k - A_{cell}v_{gas,out}^k \frac{\phi^k}{1+\phi^T} - \left(Q_{feed}-Q_{out}\right)\phi^k\right) \quad k = 1,\ldots,K, \tag{6}$$

where $\phi^T = \sum_{k=1}^{K}\phi^k$.

In the original model, the tailings flowrate (Q_{tails}) was modelled assuming that the pulp height was controlled via a valve (Equation 12 in Quintanilla et al. (2021c)), as proposed by Jämsä-Jounela et al. (2003). In the present study, we have defined tailings flowrate in terms of a Proportional–Integral (PI) controller equation to make it more generic. The controller goal is to maintain a pulp height setpoint (h_p^{SP}). The derivation of the PI controller yields:

$$\frac{dQ_{tails}}{dt} = k_p\frac{dh_p}{dt} + \frac{k_p}{\tau_i}e, \tag{7}$$

where the error was defined as:

$$e(t) = h_p - h_p^{SP}. \tag{8}$$

The proportional constant (k_p) used for this study was 0.1 $m^2 s^{-1}$ and the integral time constant (τ_i) was 50 s.

Finally, two algebraic equations were added to solve the algebraic loop presented in the dynamic model between v_g^*, α, and α^*. Eqs. (9) and (10) are equated to zero when solving the DAE system.

$$f_{alg_1} = \alpha - \frac{v_f l_{lip} h_{over}}{Q_{air}} \tag{9}$$

$$f_{alg_2} = v^* - \frac{dh_p}{dt} - v_g^{\text{total}} \tag{10}$$

3.2. Model normalisation

The state variables were normalised to avoid failure in convergence due to differences in the order of magnitude of the different states. Further, the normalisation added robustness and rapidness to the solver convergence. To carry out the normalisation, five constants were defined in terms of the initial states ($M_{i_0}, \phi_0, h_{p_0}, Q_{tails_0}$), and the total time of prediction (t_f), as shown in Table 3.

The normalised DAE model used for the control problem is given by Eqs. (9) and (15) (algebraic equations) and Eqs. (11)–(14) (differential equations) as follows:

Normalised mass balance for each mineralogical class i:

$$\frac{d\widetilde{M}_i}{d\tilde{t}} = k_{M_i}\left(m_{feed_i} - m_{\text{tails}\ i} - m_{TF_i} - m_{ENT_i}\right) \quad i = 1,\ldots,I. \tag{11}$$

Normalised gas holdup for each bubble size class k:

$$\frac{d\widetilde{\phi^k}}{d\tilde{t}} = k_\phi\left(\frac{1+\phi^T}{A_{cell}h_p}\left(Q_{air}d_{b_{prop}}^k - A_{cell}v_{gas}^k\frac{\phi^k}{1+\phi^T} - \left(Q_{feed}-Q_{out}\right)\phi^k\right)\right) \quad k = 1,\ldots,K. \tag{12}$$

Normalised pulp height:

$$\frac{d\widetilde{h_p}}{d\tilde{t}} = k_{h_p}\left(Q_{feed} - Q_{out} + Q_{air} - A_{cell}v_{gas,out}^{\text{total}}\right) \tag{13}$$

Normalised tailings flowrate:

$$\frac{d\widetilde{Q_{\text{tails}}}}{d\tilde{t}} = k_{Q_{\text{tails}}}\left(\frac{k_p}{k_{h_p}}\frac{d\widetilde{h_p}}{d\tilde{t}} - \frac{k_p}{\tau_i}e\right), \tag{14}$$

where $\widetilde{\bullet}$ refers to normalised variables (states and time). Note that the normalised time $\tilde{t} = t/t_f \in [0,1]$. Additionally, the algebraic Eq. (10) had to be normalised as well since it is a function of $\frac{d\widetilde{h_p}}{d\tilde{t}}$. This yields:

$$f_{alg_{\alpha_f}} = k_{h_p}\left(v_g^* - v_g^{\text{total}}\right) - \frac{d\tilde{h}_p}{d\tilde{t}}. \tag{15}$$

4. Sensitivity analyses for the objective function

Sensitivity analyses were performed to select an effective objective function for the control problem. The E-MPC strategy proposed in this study considers a rougher froth flotation cell, which aims to recover as much valuable metal as possible while complying with a minimum concentrate grade. This means that the ultimate objective of the dynamic optimisation problem is to maximise metallurgical recovery, which is defined as the fraction of total valuable metal contained in the feed that is recovered in the concentrate. Metallurgical recovery can be calculated using Eq. (16), where $M_{metal,\text{conc}}$ is the mass of metal (copper in this study) in the concentrate, and $m_{metal,\ \text{feed}}$ is the mass of metal in the feed.

$$\text{Rec} = \frac{M_{\text{metal,conc}}}{m_{\text{metal,\ feed}}}. \tag{16}$$

The mass of metal ($M_{metal,\text{conc}}$) in the concentrate can be calculated using first-principle models (see Equations 51 and 56 in Quintanilla et al. (2021c)). However, it is worth mentioning that metallurgical recovery is only meaningful at steady state, as it compares how much metal is recovered in the concentrate versus how much metal entered the feed after a certain residence time (i.e. it is not instantaneous). For this reason, in this study, the objective function (Eq. (20)) of the dynamic optimisation strategy evaluates recovery only at a final time (t_f), assuming that a steady state is reached. Therefore, the objective function should include more information coming from process variables that (1) are dynamic, (2) ideally, can be estimated in real-time, and (3) contribute to maximising the metallurgical recovery. These three characteristics can be found in two flotation variables: air recovery and concentrate grade.

Air recovery is a measure of froth stability that is defined as the fraction of air that enters a flotation cell that overflows as unburst bubbles. Air recovery can be calculated using the overflowing froth velocity (v_f), froth height above the cell lip (h_{over}), lip length (l_{lip}), and the inlet air flowrate (Q_{air}), as follows:

$$\alpha = \frac{v_f\ l_{lip}\ h_{over}}{Q_{air}} = \frac{A_{cell}\ v_f\ l_{lip}\ h_{over}}{j_g}. \tag{17}$$

Air recovery is directly linked to flotation performance. Hadler and Cilliers (2009) demonstrated that the best flotation performance is obtained when a peak in air recovery (PAR) is found, as shown schematically in Fig. 6. At air flowrates lower than PAR air flowrate, bubbles tend to be heavily loaded, with froth moving slowly but steadily. These froths produce low air recovery and metallurgical recovery, but high concentrate grades. On the contrary, air flowrates beyond PAR air flowrate cause bubbles to be under-loaded, resulting in unstable froths that burst quickly. These froths result in reasonably high metallurgical recoveries, but low concentrate grades (Hadler et al., 2010).

Air recovery can be measured using an optical laser to measure the froth height above the lip, and a camera (or more than one) to measure overflowing froth velocity (e.g. via a block-matching image analysis). Since air recovery is a non-intrusive, reliable indicator of froth stability and gives dynamic information on the performance of the cell, it is a sensible variable to incorporate into the objective function.

Table 3
Normalisation parameters for the ODEs in the dynamic model in Quintanilla et al. (2021c).

ODE	Normalisation parameter
Mass balance for each mineralogical class i (Equation 9 in Quintanilla et al. (2021c))	$k_{\mathrm{i}} = \frac{t_f}{M_{\mathrm{i}}^0}$
Gas holdup for each bubble size class k (modified - See Eq. (6))	$k_{\phi} = \frac{t_f}{\phi_0}$
Pulp height (Equation 22 in Quintanilla et al. (2021c))	$k_{h_p} = \frac{t_f}{h_p^0}$
Tailings flowrate (modified - See Eq. (7))	$k_{Q_{\mathrm{tails}}} = \frac{t_f}{M_{Q_{\mathrm{tails}}}^0}$

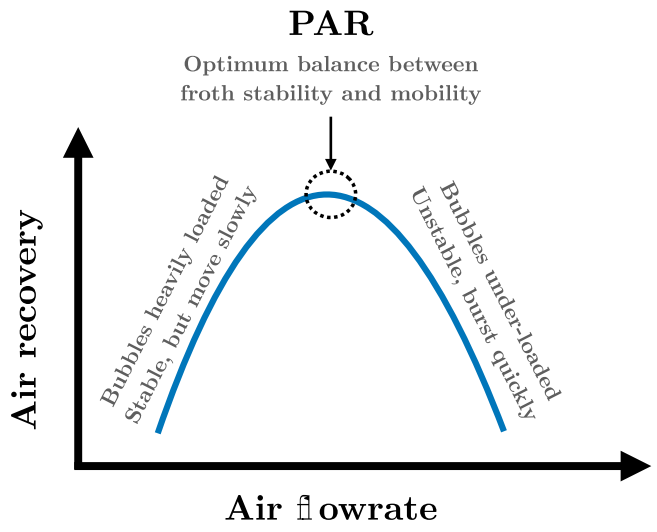

Fig. 6. Schematic showing the evolution of air recovery (blue line) as a function of air flowrate. Adapted from Hadler et al. (2010) and Shean et al. (2017). (For interpretation of the references to colour in this figure legend, the reader is referred to the web version of this article.)

To this end, a sensitivity analysis was carried out to assess the effect of the decision variables (Q_{air}^{SP} and h_p^{SP}) on air recovery. In other words, by varying the air flowrate and pulp height setpoints, this sensitivity analysis enables quantifying the magnitude and direction of changes in air recovery. Note that the superficial air velocity j_g is used instead of Q_{air} since it is comparable between flotation cells of different sizes and is therefore widely used in the minerals processing community. As shown in Fig. 7, air recovery is highly sensitive to air flowrate, as expected. However, with the current models available for air recovery, it is relatively insensitive to the other decision variable, pulp height, leaving room for incorporating more information into the objective function. It is worth mentioning that pulp height was considered in the optimisation problem because it is measured online in most flotation cells. Thus, further sensitivity analyses for metallurgical recovery and concentrate grade were performed to assess their sensitivity to pulp height.

The concentrate grade is the mass concentration of metal in the concentrate which, unlike metallurgical recovery, is meaningful in a dynamic state. As shown in Eq. (18), the concentrate grade can be calculated as the mass of metal in the concentrate divided by the total mass of solids in the concentrate.

$$\text{Grade} = \frac{M_{\text{metal , conc}}}{M_{\text{total, conc}}}. \tag{18}$$

The sensitivity analyses displayed in Figs. 8 and 9 reveal that both metallurgical recovery and concentrate grade are highly sensitive to both decision variables. It can also be observed that, as expected, there is a clear trade-off between metallurgical recovery and grade. That is to say, while higher grades can be achieved for lower pulp heights (i.e. froth depth increases), this results in the lowest metallurgical recovery. Since metallurgical recovery is only meaningful at a steady state, an indirect way to maximise recovery during the dynamic state is by minimising the concentrate grade up to a certain limit. Hence, another sensible term to be included in the objective function is the minimisation of the concentrate grade, restricting it to a minimum value, with 20% used in this study (Eq. (26)). While the 20% grade requirement is a sensible value, the actual number that a plant might use would depend upon its specific technical and economic requirements and could therefore, ultimately, form part of plant scale economic optimisation, with this value being cascaded to the control of the individual cell via the method outlined in this paper. Further simulations of the proposed control strategy for different minimum concentrate grades can be found in the Supplementary Material.

After the sensitivity analyses shown above, it was decided to implement the E-MPC using the objective function shown in Eq. (20). Additionally, since the concentrate grade is not usually measured online for individual cells in most flotation plants, simulations were performed to evaluate the effect of air recovery alone on the final metallurgical recovery, i.e. without adding the concentrate grade and metallurgical recovery in the objective function.

5. Dynamic optimisation formulation

The optimal control problem (OCP) of dynamic optimisation has been formulated using nonlinear programming (NLP). The general form for the NLP using orthogonal collocations (i.e. full discretisation), and normalised variables $(\tilde{\bullet})$, is:

$$\begin{aligned} \underset{\tilde{\mathbf{x}}(t)\in\mathbb{R}^{N_x},\mathbf{u}_n\in\mathbb{R}^{N_u},n=0,\ldots,N_p-1,\tilde{\mathbf{z}}(t)\in\mathbb{R}^{N_z}}{\text{maximise}} \quad & \boldsymbol{J}(\tilde{\mathbf{x}},\mathbf{y},\tilde{\mathbf{z}},\mathbf{u},\boldsymbol{\beta},t_{N_P}) \\ \text{s.t.} \quad & \mathbf{h}(\tilde{\mathbf{x}},\mathbf{y},\tilde{\mathbf{z}},\mathbf{u},\mathbf{p},\tilde{t}) = 0 \quad \tilde{t}\in[t_0,t_{N_p}] \\ & \mathbf{g}(\tilde{\mathbf{x}},\mathbf{y},\tilde{\mathbf{z}},\mathbf{u},\mathbf{p},\tilde{t}) \le 0 \quad \tilde{t}\in[t_0,t_{N_p}] \\ & \mathbf{u}(t) = \mathbf{u}_n \quad \tilde{t}\in[t_n,t_{n+1}] \quad n=0,\ldots,N_p-1 \end{aligned} \tag{19}$$

where the normalised time limits are $t_0 = 0$, $t_{N_p} = 1$, and:

$\tilde{\boldsymbol{x}}^T := \left[\widetilde{M}_i, \tilde{\phi}^k, \tilde{h}_p, \tilde{Q}_{\text{tails}}\right]$
$\boldsymbol{y}^T := \left[\alpha, G_{\text{conc}}, \text{Rec}\right]$
$\tilde{\mathbf{z}}^T := [\alpha, \alpha^*]$
$\boldsymbol{u}^T := \left[Q_{\text{tails}}, h_p^{SP}\right]$
$\boldsymbol{h}$: Dynamic model found in Quintanilla et al. (2021c) (normalised models in Eqs. (9), (11)- (15)).
$\boldsymbol{g}$: Process constraints (Eqs. (25) – (26)),

where α is air recovery, G_{conc} is the concentrate grade, Rec is the metallurgical recovery, and $\mathbf{u}_j$ for $j = 1, 2$, are the control inputs (decision variables) defined in Eq. (22). After conducting sensitivity analyses in Section 4, it was concluded that a robust objective function for maximising the performance of a rougher flotation cell should include three variables: (1) the dynamics of air recovery (as a measure of froth stability), (2) the dynamics of concentrate grade (calculated through first principles), and (3) the maximisation of metallurgical recovery

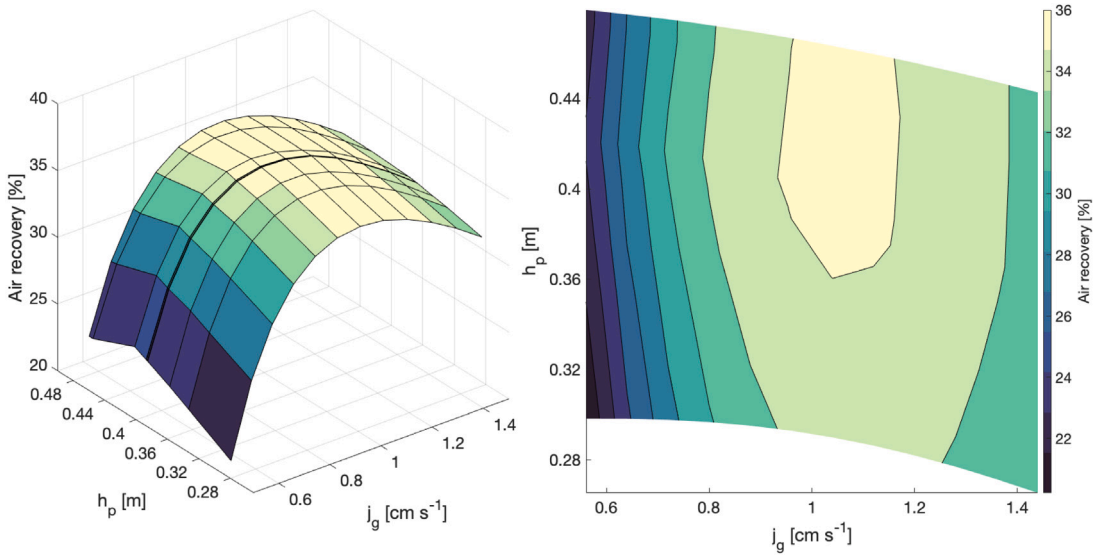

Fig. 7. Sensitivity analysis of air recovery in terms of the two decision variables: air flowrate ($Q_{air} = A_{cell} j_g$) and pulp height (h_p) at steady state.

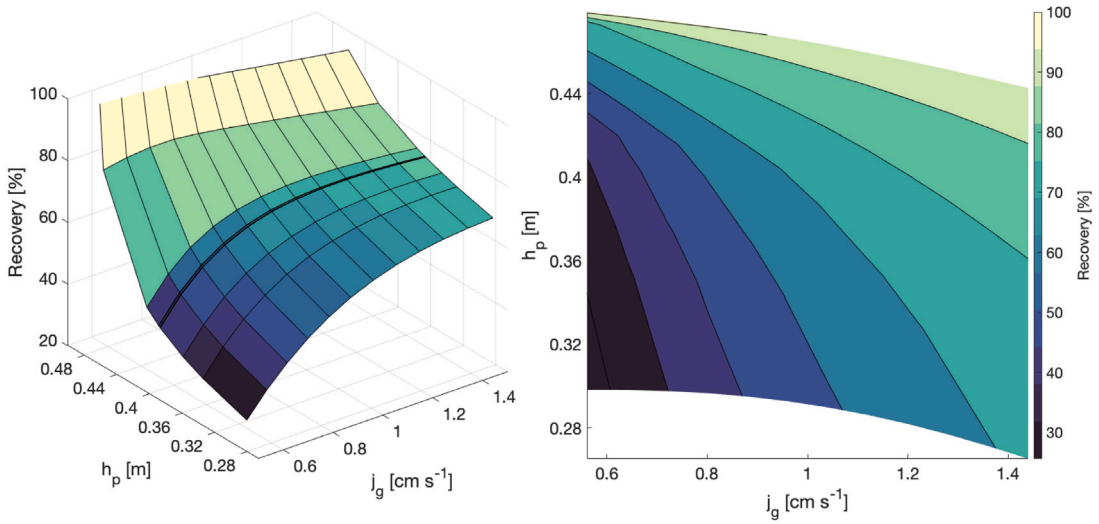

Fig. 8. Sensitivity analysis of metallurgical recovery in terms of the two decision variables: air flowrate ($Q_{air} = A_{cell} j_g$) and pulp height (h_p) at steady state.

at the end of the prediction horizon (assuming that steady-state is reached). These three variables contribute to taking full advantage of both decision variables. However, due to the trade-off between grade and recovery, the concentrate grade is minimised in the objective function but constrained to a minimum value, as previously discussed. Additionally, minimising control effort is also considered in the objective function to avoid oscillations. The resulting objective function, denoted by J, is expressed as follows:

$$J := \int_{t_0}^{t_{N_p}} (\beta_\alpha \alpha(t) - \beta_{Grade} G_{conc}(t)) dt + \beta_{\text{Rec}} \text{Rec}\left(t_{N_p}\right) - \sum_{n=0}^{N_p-1} \left(\Delta \mathbf{u}_n^T \boldsymbol{\beta}_{\mathbf{u}} \Delta \mathbf{u}_n\right). \tag{20}$$

Each term is penalised by a parameter such that:

$$\boldsymbol{\beta}_{\mathbf{u}} := \begin{bmatrix} \beta_{u_1} & 0 \\ 0 & \beta_{u_2} \end{bmatrix}, \tag{21}$$

where:

$$\boldsymbol{\beta}^T := [\beta_\alpha, \beta_{G_{\text{conc}}}, \beta_{\text{Rec}}, \beta_{u_1}, \beta_{u_2}] = [10^8, 10^6, 10^8, 10^6, 10^2].$$

The selection of the values for the vector $\boldsymbol{\beta}$ was supported by a parametric sensitivity analysis. Under the operating conditions analysed in this study, these selected values for $\boldsymbol{\beta}$ led to the optimal performance of the optimisation solver in terms of convergence time.

The economic performance in a froth flotation cell can be measured through the metallurgical recovery (Rec in Eq. (16)) at the final time, assuming that a steady state is reached. To achieve this, dynamic air recovery (α in Eq. (17)) is maximised, as it has been demonstrated that operating froth flotation cells at high air recoveries improve metallurgical performance (Hadler and Cilliers, 2009).

The terms $\Delta \mathbf{u}_n$ represent the control efforts, which are defined as:

$$\Delta \mathbf{u}_n = \mathbf{u}_n - \mathbf{u}_{n-1}, \quad n = 0, \ldots, N_c - 1, \tag{22}$$

It is always assumed that the first values for the control variables are known. Thus, $\mathbf{u}_{-1}$ in Eq. (22) was defined as $\mathbf{u}_{-1} = [Q_{air}^{SP_0}, h_p^{SP_0}]$.

By definition, the control variables must not change after the control horizon; therefore, Eq. (23) was imposed:

$$\Delta \mathbf{u}_n = 0, \quad n = N_c, \ldots, N_p - 1, \tag{23}$$

where N_c is the number of control intervals.

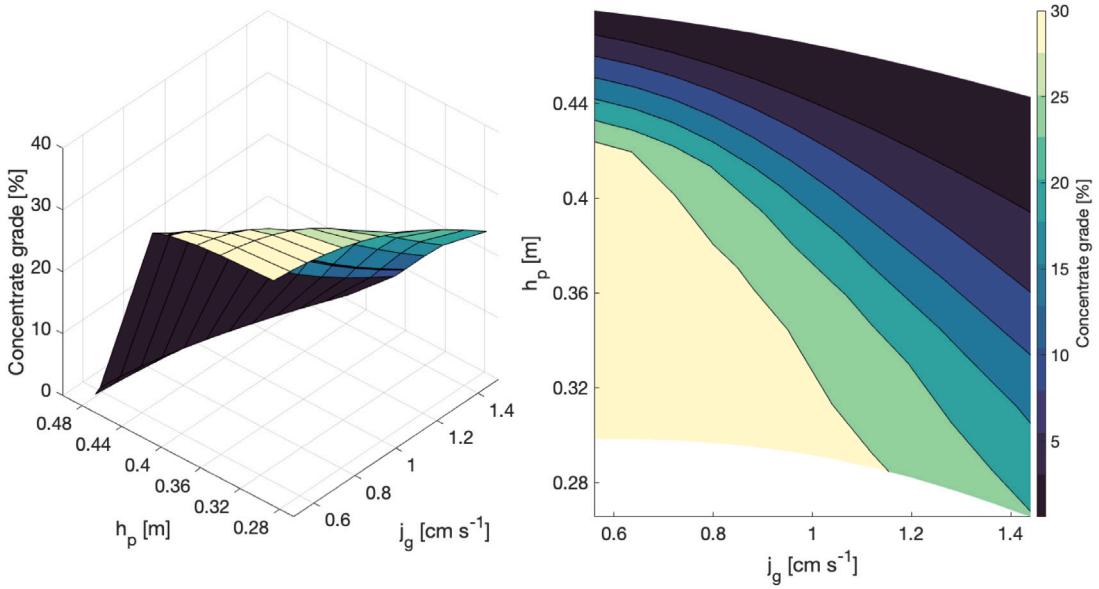

Fig. 9. Sensitivity analysis of concentrate grade in terms of the two decision variables: air flowrate ($Q_{air} = A_{cell} j_g$) and pulp height (h_p) at steady state.

Note that $\Delta t = t_f / N_p$, and the normalised $\Delta \tilde{t}$ is $\Delta t / t_f$. Hence, $\Delta \tilde{t} = 1/N_p$. Additionally:

$$\tilde{t}_{n+1} = \tilde{t}_n + \Delta \tilde{t} \quad n = 0, \ldots, N_p - 1. \tag{24}$$

Constraints were imposed for all states $\tilde{\mathbf{x}}$, control variables $\mathbf{u}$, and algebraic variables $\tilde{\mathbf{z}}$ to ensure that they are physically consistent:

$$\begin{aligned} \tilde{\mathbf{x}}_{\mathbf{lb}} &\leq \tilde{\mathbf{x}} \leq \tilde{\mathbf{x}}_{\mathbf{ub}} \\ \mathbf{u}_{\mathbf{lb}} &\leq \mathbf{u} \leq \mathbf{u}_{\mathbf{ub}} \\ \tilde{\mathbf{z}}_{\mathbf{lb}} &\leq \tilde{\mathbf{z}} \leq \tilde{\mathbf{z}}_{\mathbf{ub}} \end{aligned} \tag{25}$$

The lower and upper bounds for the states and algebraic variables were normalised with the respective initial state for each iteration. Since E-MPC is applied following a receding horizon strategy, the vectors $\tilde{\mathbf{x}}_{\mathbf{lb}}$, $\tilde{\mathbf{x}}_{\mathbf{ub}}$, $\tilde{\mathbf{z}}_{\mathbf{lb}}$ and $\tilde{\mathbf{z}}_{\mathbf{ub}}$ must be updated in every iteration with a new vector of state variables. The lower and upper limits of the control variables ($\mathbf{u}_{\mathbf{lb}}$ and $\mathbf{u}_{\mathbf{ub}}$) were limited to a predefined range of changes with respect to their current value at each iteration: changes by up to 100% for Q_{air}^{SP} and 10% for h_p^{SP}. Additionally, another constraint was imposed to ensure a minimum concentrate grade of 20% (Eq. (26)). This is because there is always a trade-off between metallurgical recovery (Rec) and concentrate grade. As discussed previously, an appropriate minimum concentrate grade value for a flotation plant depends on its technical and economic needs and can be determined through plant-scale economic optimisation. Additional simulations for various minimum concentrate grades are available in the Supplementary Material.

$$G_{conc} \geq 0.2 \tag{26}$$

Other considerations for the implementation of the optimal control problem are listed below:

1. Data from the experiments carried out in Quintanilla et al. (2021b) for model calibration and validation were used as initial states and control variables. This means that there are nine different operating conditions in total (full factorial design of 3^2), which correspond to three levels of superficial air velocity j_g: 0.5, 0.7, and 0.9 cm s^{-1} and three levels for the tailings valve position (which will define the initial pulp height): 25%, 37.5%, and 50% open. Additionally, other relevant parameters, such as tank dimensions and operating condition ranges, were the same as those used for model calibration and validation.
2. Two mineralogical classes were assumed: chalcopyrite (the valuable mineral that contains 34.5% of copper) and quartz (gangue). It was assumed that particle sizes and floatability were constant.
3. Total time of prediction (t_f) was 600 s because the experimental rig used for the model validation reached steady-state at about 10 min (settling time).
4. Number of prediction intervals (N_p) was 10, and number of control intervals (N_c) was 3. Each time step, Δt was equalled to $\frac{t_f}{N_p} = 60$ s.

The dynamic optimisation problem presented here from Eq. (19) to Eq. (26) was implemented using CasADi by solving the OCP using orthogonal collocations as the discretisation method using automatic differentiation, as explained in Section 2.3.

6. E-MPC results and discussions

Fig. 10 displays the evolution of air recovery, α, and the control variable Q_{air} (represented as j_g) over time. As can be seen from Fig. 10, α is always maximised until it reaches a peak in all cases. The control sequences for superficial air velocity seem to have a similar trend, i.e. increasing superficial air velocity until a maximum is reached, followed by a gradual reduction of its value. It is expected that air recovery reaches a peak for a certain superficial air velocity when pulp height is constant. However, it is not the case for this study as pulp height is the other control variable that changes over time in order to maximise the objective function of Eq. (20). As was demonstrated in the sensitivity analysis (Section 4), air recovery not only depends on j_g but also on pulp height. For the first time, air recovery is included in a dynamic optimisation strategy, which is an excellent option for the majority of current industrial flotation cells, as it is a reliable and non-intrusive technique for measuring froth stability online (Hadler et al., 2010). Moreover, as mentioned before, it has been demonstrated that air recovery is directly linked to froth flotation performance (improvements in concentrate grade and metallurgical recovery).

As shown in Fig. 11, in all cases the pulp heights decrease until reaching a lower limit. It can be observed that the pulp height in the process is not the same as the pulp height setpoint, particularly for the first three steps. These differences are due to the fact that the pulp height is controlled by manipulating the tailings flowrate, which was simulated as a PI controller (Eq. (7)). It must be emphasised that the

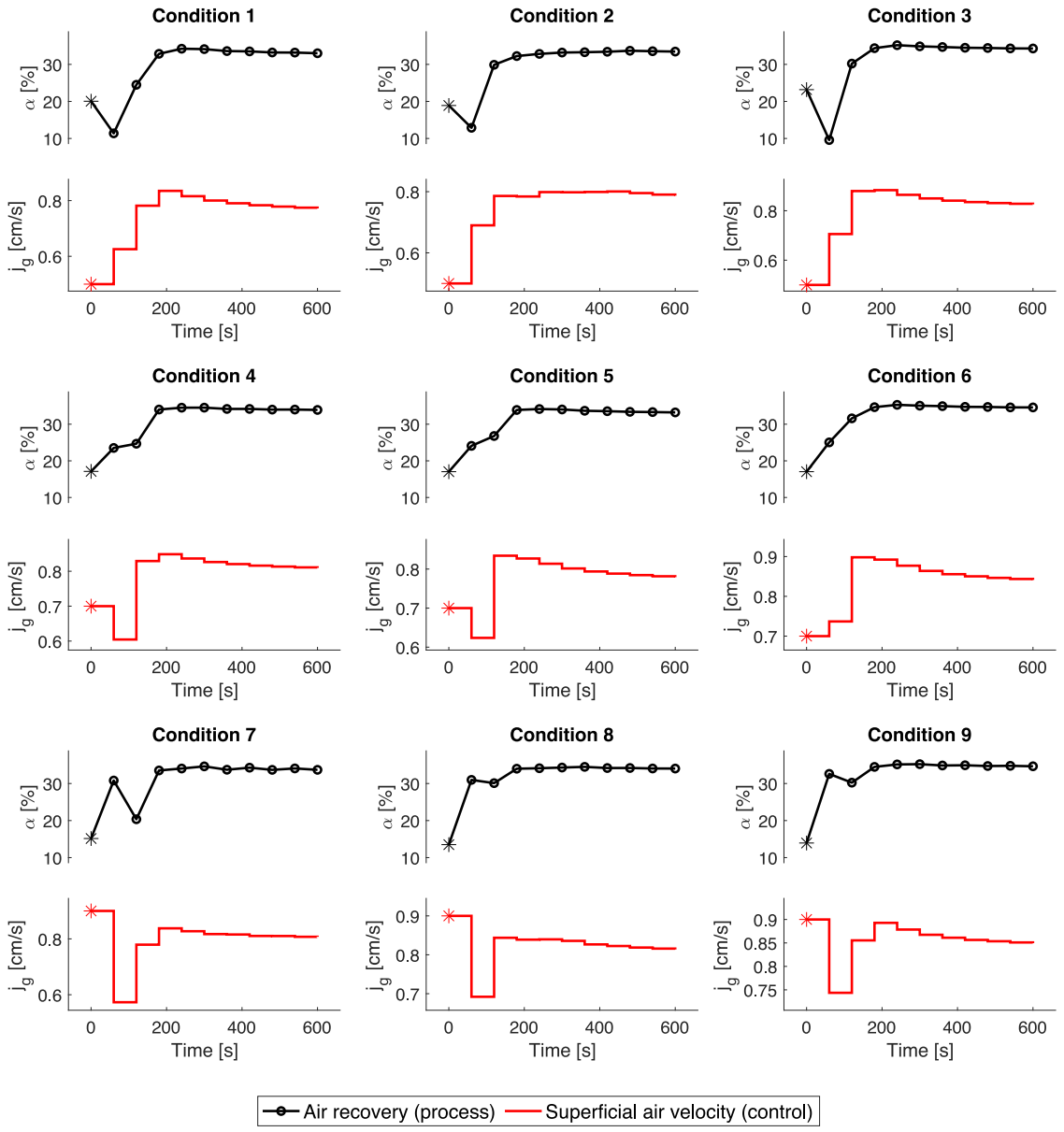

Fig. 10. Air recovery (α) and superficial air velocity (j_g) over time for the E-MPC implementation for the nine different operating conditions used as starting points in the simulations (rows 1–3: j_{g_0} = 0.5, 0.7 and 0.9 cm s^{-1}, respectively; columns 1–3: tailings valve = 25%, 37.5% and 50% open, respectively). The asterisks are the initial values of air recovery and j_g (i.e. $t = 0$) for each operating condition. The black circles are the air recovery values in the process (simulated) and the red stairs are the control sequences for superficial air velocity (j_g). (For interpretation of the references to colour in this figure legend, the reader is referred to the web version of this article.)

tuning parameters of any PI controller are never perfect, and there is a time delay in the regulatory control layer (see Fig. 1) before it can reach the setpoint sent to it by the upper optimisation layer. Note that, in this study, supervisory control and optimisation layers are combined in a single layer: E-MPC. A noticeable improvement in metallurgical recovery was achieved in all cases. In Fig. 12, the transition from one steady-state ($t = 0$) to another ($t = t_f$) is shown in the top graphs of each condition for the recoveries (blue dots), while the dynamic grade is shown on the bottom (black curves). From the figure, it can be seen that the concentrate grade always goes towards its limit in all cases, as expected.

Overall, the controller manipulates the Q_{air} setpoints (denoted as superficial air velocity in Fig. 10), ranging from 0.77 cms^{-1} (condition 1) to 0.84 cms^{-1} (condition 6) at $t = 600$ s. In contrast, the pulp height setpoints reach the lowest boundary in all conditions. The behaviour of the pulp height setpoints may be due to the range of movement for the pulp setpoint not being very large, since we are simulating a laboratory-scale cell (there is a difference of 5.5 cm between the upper and lower limits). Hence, lower pulp heights (i.e. deeper froths) might be necessary to achieve or maintain a 20% concentrate grade in the conditions assessed in this study. To further generalise this point, additional simulations were performed with the pulp height constraint relaxed. The Supplementary Material contains the results of the simulations comparing different pulp height lower bounds for the middle condition (condition 5), as well as simulations without pulp height constraints in all conditions. It was concluded that the controller found different solutions when the lower bound changed, but did not hit it in every case. Furthermore, even though metallurgical

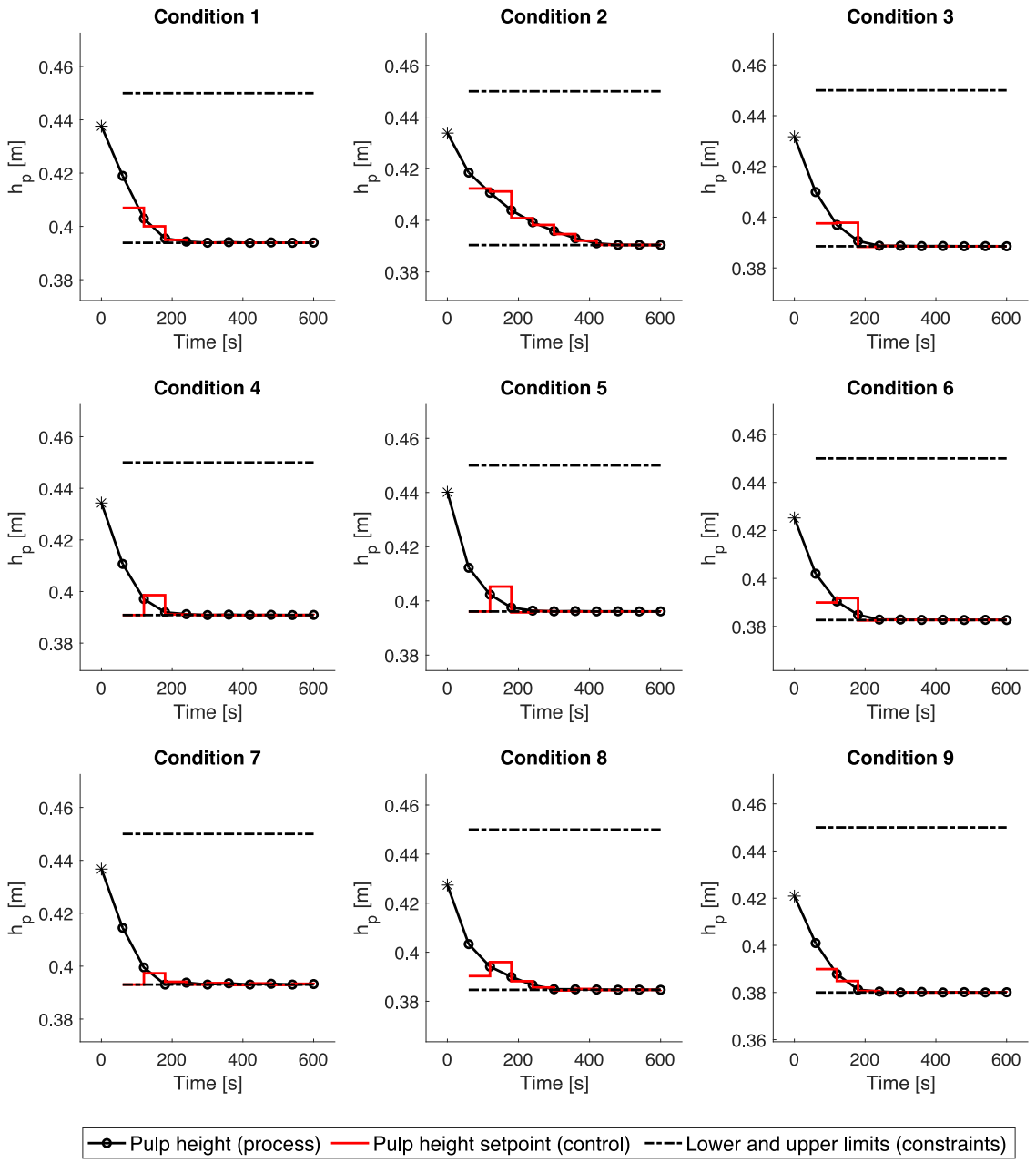

Fig. 11. Pulp height (simulated) and pulp height setpoint (control variable) over time for the E-MPC implementation for the nine different operating conditions used as starting points in the simulations (rows 1–3: j_{g_0} = 0.5, 0.7 and 0.9 cm s^{-1}, respectively; columns 1–3: tailings valve = 25%, 37.5% and 50% open, respectively). The asterisks are the initial values of pulp height (i.e. t = 0) for each operating condition. The black circles are the pulp height values in the process (simulated) and the red stairs are the control sequences for the pulp height setpoints. (For interpretation of the references to colour in this figure legend, the reader is referred to the web version of this article.)

recoveries without pulp height constraints were higher than those with constraints, this does not necessarily indicate what actually occurs within a flotation cell, as a low pulp height may indicate the froth is not overflowing, which is undetected by the controller. Therefore, it is essential to impose a constraint on the minimum pulp height.

It is clear that economic improvements can be achieved by implementing E-MPC. It can be seen from Fig. 12 that recovery improvements as high as 22% can be achieved (e.g. condition 4) from one steady state to another, based on the laboratory-scale data considered in this study. It is also interesting to note that the dynamic optimisation can easily handle the concentrate grade constraint in all cases, even when the initial grade was below 20% (e.g. condition 7 in Fig. 12). Additionally, this figure illustrates the evolution of the simulated metallurgical recovery over time, which confirms the assumption that a steady state is reached after 600 s in all the conditions.

In parallel, an E-MPC strategy using Eq. (27) as an objective function was implemented for the same nine conditions to compare their performance.

$$J_1 := \beta_\alpha \int_{t_0}^{t_f} \alpha \, dt - \sum_{n=0}^{N_p-1} \left(\beta_{u_1} \Delta u_1^2 (t_n) + \beta_{u_2} \Delta u_2^2 (t_n) \right). \tag{27}$$

In this new objective function, neither metallurgical recovery nor concentrate grade was considered. The results using Eq. (27) as an objective function revealed that the final metallurgical recovery was between 1 to 2% lower than the first E-MPC results (objective function

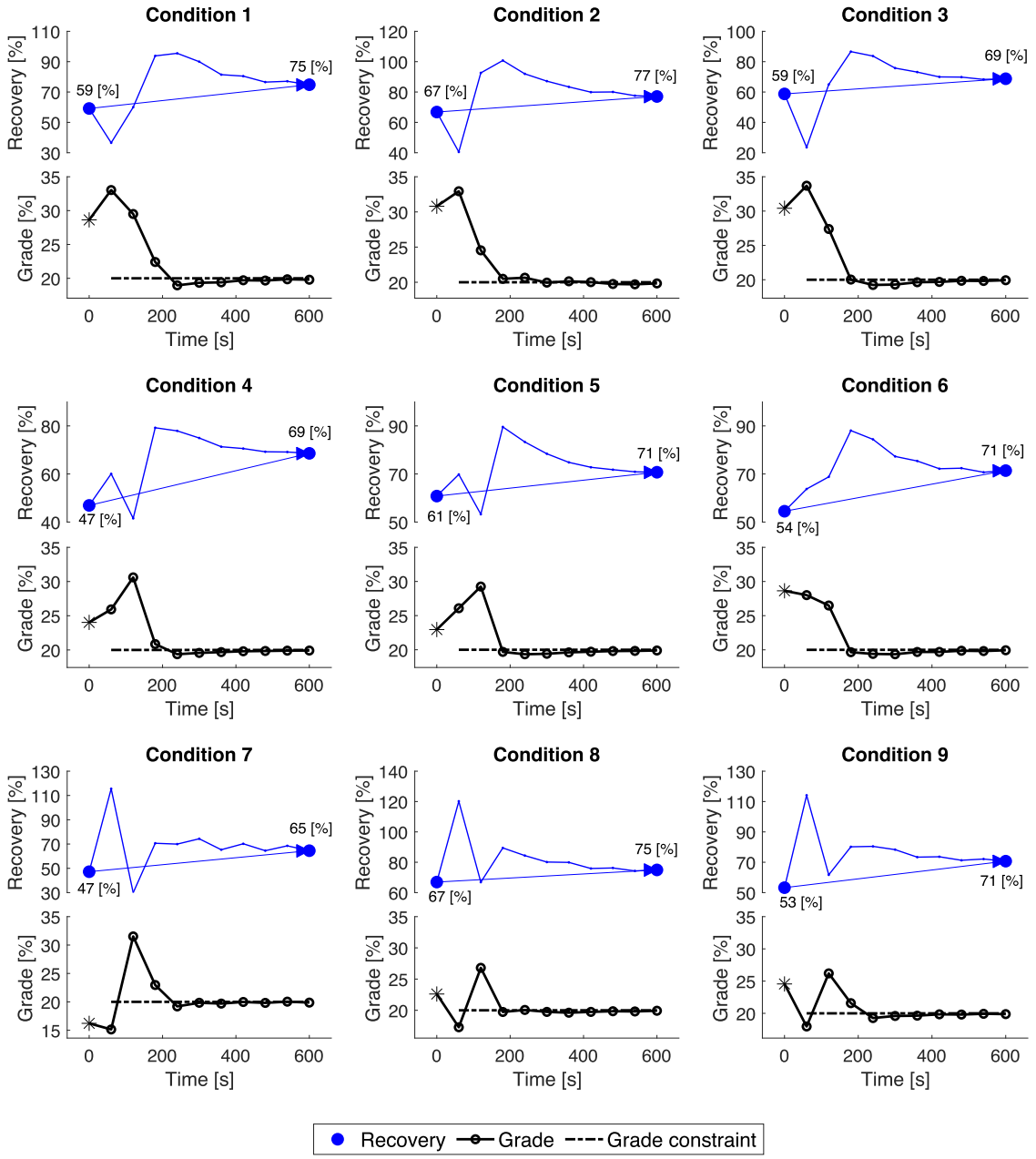

Fig. 12. Recovery (blue) and concentrate grade (black) for the nine different operating conditions (rows 1–3: j_{g_0} = 0.5, 0.7 and 0.9 cm s^{-1}, respectively; columns 1–3: tailings valve = 25%, 37.5% and 50% open, respectively). Recovery is shown only from one steady state (first blue dot) to another steady state (second blue dot) because, by definition, it has no meaning in a dynamic state. (For interpretation of the references to colour in this figure legend, the reader is referred to the web version of this article.)

shown in Eq. (20)). While these results seem to be fairly similar, undoubtedly, the differences are significant as even small improvements in efficiency will lead to great economic impacts for a large-scale process such as froth flotation.

For illustrative purposes and to have an estimate of how the economics of the process improves when the metallurgical recovery is maximised, a net smelter return formula (Eq. (28)) was evaluated at steady-state. This economic function, which was first suggested by Schena et al. (1996), has been used in different optimisation applications, such as those found in Hu et al. (2013), Jamett et al. (2015), Liang et al. (2020). However, it should be noted that a rougher flotation cell, such as the one studied here, has a final goal to recover as much mineral as possible for a certain concentrate grade. The concentrate flow is typically sent to a cleaning stage within the flotation circuit, which has as an objective to increase concentrate grade. This means that the smelter return formula is appropriate to optimise flotation circuits rather than a single flotation cell and, for this reason, it was not included in the objective function of the dynamic optimisation for one single flotation cell.

$$\text{Revenue} = Q_c p \left(G_{\text{conc}} - u\right)(q - Rfc) - Q_c \,\text{Trc}\,. \tag{28}$$

Q_c is the concentrate flowrate, G_{conc} is the concentrate grade, and p, u, q, Rfc and Trc are parameters. The value of each parameter can be found in the original Ref. Schena et al. (1996). Taking into consideration that all nine conditions are those carried out at a laboratory scale, an increment of 1% in the metallurgical recovery produced a profit improvement of about 600 to 900 $/h, depending on the operating conditions and the concentrate grade. Overall, these results confirm

the importance of implementing advanced control techniques, such as E-MPC, in the froth flotation process, using an adequate objective function.

7. Conclusions

In this study, we implemented the first economic model predictive control (E-MPC) for a froth flotation cell using a phenomenological dynamic model that includes froth physics. The dynamic model is a DAE system that was previously calibrated and validated with experimental data. The same experimental data were used as initial conditions for the implementation of the E-MPC strategy, using orthogonal collocations with automatic differentiation via CasADi. Four model equations were modified from the original dynamic flotation model to facilitate the calculation of derivatives as well as to avoid numerical problems. Furthermore, to improve convergence and add robustness, the variables of the dynamic model (states and time) were normalised, leading to a feasible implementation strategy in terms of computational time.

Sensitivity analyses were performed to select the best objective function for the dynamic optimisation, which has as an ultimate goal of maximising the metallurgical recovery at a steady state, subject to a minimum concentrate grade constraint. These analyses indicated that the best use of the two control variables (air flowrate and pulp height setpoints) is achieved by incorporating air recovery, metallurgical recovery and concentrate grade in the objective function.

The E-MPC implementation results revealed that this strategy led to substantial increments in metallurgical recovery, as high as 22% from one steady-state to another, based on laboratory-scale data. Further E-MPC simulations were carried out to assess the effect of including only air recovery in the objective function, as it can be more easily measured online than metallurgical recovery or concentrate grade. The results showed that maximising air recovery alone led to metallurgical recoveries between 1 to 2% lower than when considering the three variables in the objective function. While the selection of variables for the objective function is shown to be crucial, even the simpler option of maximising air recovery represents a good control strategy. Our results thus provide compelling evidence that confirms the substantial benefits of implementing an advanced control technique, such as E-MPC, in the froth flotation process.

Future work will focus on the assessment of the proposed E-MPC strategy in a laboratory-scale froth flotation bank, as the one described in Quintanilla et al. (2023), to mimic what can be found at the industrial scale. Disturbances in the process, such as changes in feed flowrate and particle size distribution, should also be included in the control strategy. To this end, a state estimator, such as the moving horizon estimator (MHE) strategy, should be implemented to improve model predictions under disturbances.

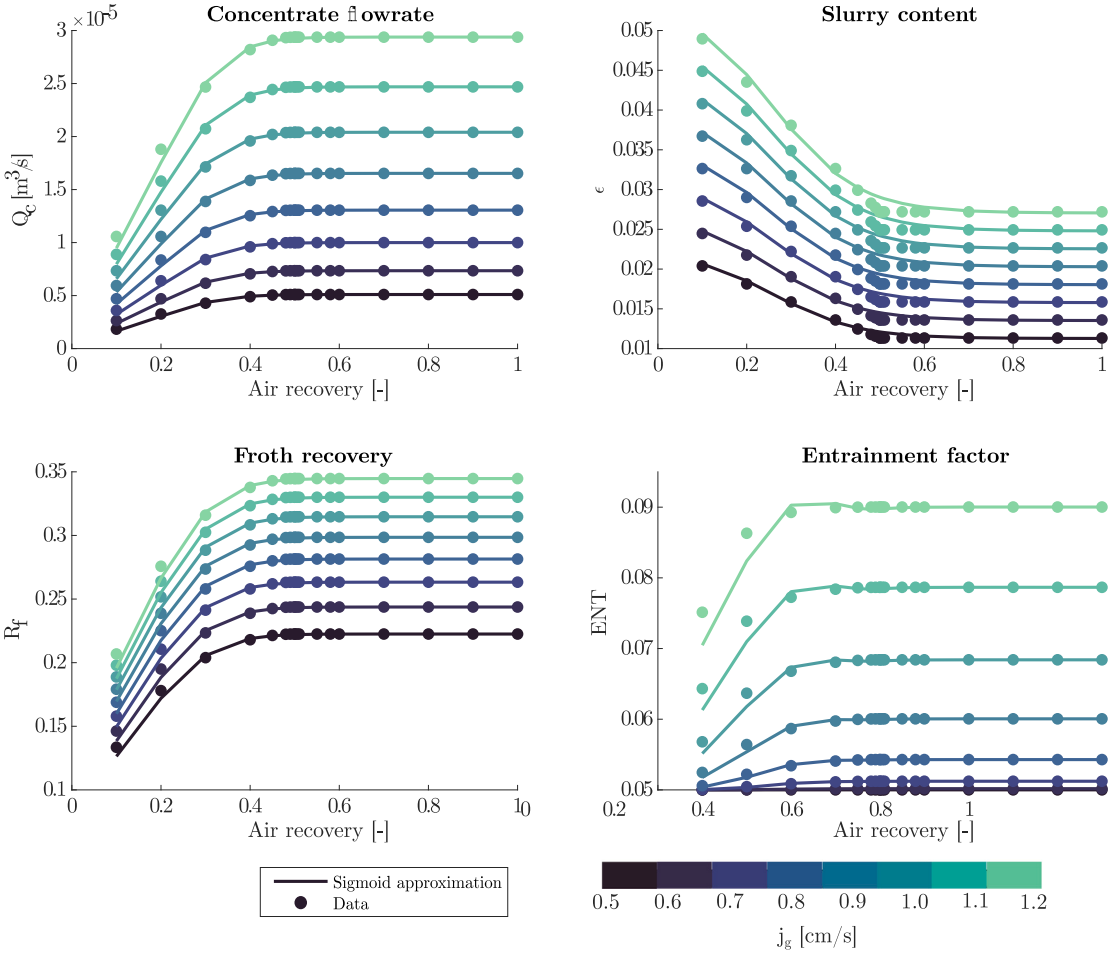

Fig. A.13. Sigmoid approximations for variables defined with *if-else* statements in the dynamic model from Quintanilla et al. (2021c): Concentrate flowrate (Q_c), slurry content (ϵ), froth recovery (R_f) and entrainment factor (ENT). They were simulated at a steady state for different values of air recovery and different values of superficial air velocities (J_g). The squared dots were calculated using the original models (*if-else* statements), while the continuous lines were calculated using the sigmoid approximations shown in Eqs. (3) and (4).

CRediT authorship contribution statement

Paulina Quintanilla: Conceptualization, Funding acquisition, Methodology, Software, Validation, Formal analysis, Investigation, Data curation, Resources, Visualization, Writing – original draft, Writing – review & editing. **Daniel Navia:** Conceptualization, Methodology, Software, Validation, Formal analysis, Writing – review & editing. **Stephen J. Neethling:** Conceptualization, Methodology, Formal analysis, Writing – review & editing, Supervision. **Pablo R. Brito-Parada:** Conceptualization, Methodology, Validation, Formal analysis, Investigation, Resources, Supervision, Writing – review & editing.

Declaration of competing interest

The authors declare the following financial interests/personal relationships which may be considered as potential competing interests: Paulina Quintanilla reports financial support was provided by National Agency for Research and Development.

Data availability

Data will be made available on request.

Acknowledgments

Paulina Quintanilla would like to acknowledge the National Agency for Research and Development (ANID) for funding this research with a scholarship from "Becas Chile".

Appendix A

A comparison of the results from the simulations using the original model (*if-else* statements) and sigmoid approximations (i.e. Eqs. (3)–(5)) are displayed in Fig. A.13 for the four variables. The simulations were carried out using the same data for model validation in Quintanilla et al. (2021b), for different levels of air recovery (α in the x-axis) and superficial air velocity (different curve colours). Note that the superficial air velocity, j_g, is defined as Q_{air}/A, where Q_{air} is the volumetric air flowrate (which is a control variable), and A is the cross-sectional area of the froth flotation cell.

As can be seen from Fig. A.13, the sigmoid approximations are highly accurate for all cases. A minimal underestimation in the entrainment factor for $\alpha < 0.3$ can be observed. However, these small discrepancies are not significant when implementing advanced control strategies, as they can be corrected through feedback control. What is even more important to notice is that in all cases the trends of the approximations are the same as those using *if-else* statements.

Appendix B. Supplementary data

Supplementary material related to this article can be found online at https://doi.org/10.1016/j.mineng.2023.108050.

The Supplementary material contains further simulations performed for different concentrate grade and pulp height constraints.

References

Amrit, R., Rawlings, J.B., Angeli, D., 2011. Economic optimization using model predictive control with a terminal cost. Annu. Rev. Control 35 (2), 178–186. http://dx.doi.org/10.1016/j.arcontrol.2011.10.011.

Andersson, J.A.E., Gillis, J., Horn, G., Rawlings, J.B., Diehl, M., 2019. CasADi: a software framework for nonlinear optimization and optimal control. Math. Program. Comput. 11, 1–36. http://dx.doi.org/10.1007/s12532-018-0139-4.

Angeli, D., Amrit, R., Rawlings, J.B., 2012. On average performance and stability of economic model predictive control. IEEE Trans. Automat. Control 57 (7), 1615–1626. http://dx.doi.org/10.1109/TAC.2011.2179349.

Beck, A., 2010. Practical methods for optimal control and estimation using nonlinear programming. In: Advances in Design and Control. pp. 91–121, chapter Optimal Co.

Bergh, L.G., Yianatos, J.B., 2011. The long way toward multivariate predictive control of flotation processes. J. Process Control 21 (2), 226–234. http://dx.doi.org/10.1016/j.jprocont.2010.11.001.

Biegler, L.T., 2007. An overview of simultaneous strategies for dynamic optimization. Chem. Eng. Process.: Process Intensif. 46 (11), 1043–1053. http://dx.doi.org/10.1016/j.cep.2006.06.021.

Biegler, L.T., 2010. Nonlinear Programming: Concepts, Algorithms, and Applications to Chemical Processes. Society for Industrial and Applied Mathematics, USA.

Billings, S.a., Fakhouri, S.Y., 1977. Indentification of Non-Linear Systems Using the Wiener Model. Technical Report. ACSE Research Report 60, Automatic Control and Systems Engineering, University of Sheffield, URL: https://eprints.whiterose.ac.uk/.

Brooks, K.S., Koorts, R., 2017. Model predictive control of a zinc flotation bank using online X-ray fluorescence analysers. IFAC-PapersOnLine 50 (1), 10214–10219. http://dx.doi.org/10.1016/j.ifacol.2017.08.1772.

Brooks, K., Munalula, W., 2017. Flotation velocity and grade control using cascaded model predictive controllers. IFAC-PapersOnLine 50 (2), 25–30. http://dx.doi.org/10.1016/j.ifacol.2017.12.005.

Camacho, E.F., Bordons, C., 2007. Model Predictive Control. p. 405. http://dx.doi.org/10.1007/978-0-85729-398-5.

Chachuat, B., Singer, A.B., Barton, P.I., 2006. Global methods for dynamic optimization and mixed-integer dynamic optimization. Ind. Eng. Chem. Res. 45 (25), 8373–8392. http://dx.doi.org/10.1021/ie0601605.

Curtis, F.E., Huber, J., Schenk, O., Wächter, A., 2012. A note on the implementation of an interior-point algorithm for nonlinear optimization with inexact step computations. Math. Program. 136 (1), 209–227. http://dx.doi.org/10.1007/s10107-012-0557-4.

Cuthrell, J.E., Biegler, L.T., 1987. On the optimization of differential-algebraic process systems. AIChE J. 33 (8), 1257–1270. http://dx.doi.org/10.1002/aic.690330804.

Diehl, M., Amrit, R., Rawlings, J.B., 2011. A lyapunov function for economic optimizing model predictive control. IEEE Trans. Automat. Control 56 (3), 703–707. http://dx.doi.org/10.1109/TAC.2010.2101291.

Ellis, M., Durand, H., Christofides, P.D., 2014. A tutorial review of economic model predictive control methods. J. Process Control 24 (8), 1156–1178. http://dx.doi.org/10.1016/j.jprocont.2014.03.010.

Engell, S., 2007. Feedback control for optimal process operation. J. Process Control 17 (3), 203–219. http://dx.doi.org/10.1016/j.jprocont.2006.10.011.

Fabien, B.C., 1998. Some tools for the direct solution of optimal control problems. Adv. Eng. Softw. 29 (1), 45–61. http://dx.doi.org/10.1016/S0965-9978(97)00025-2.

Hadler, K., Cilliers, J.J., 2009. The relationship between the peak in air recovery and flotation bank performance. Miner. Eng. 22 (5), 451–455. http://dx.doi.org/10.1016/j.mineng.2008.12.004.

Hadler, K., Smith, C.D., Cilliers, J.J., 2010. Recovery vs. mass pull: The link to air recovery. Miner. Eng. 23 (11–13), 994–1002. http://dx.doi.org/10.1016/j.mineng.2010.04.007.

Heidarinejad, M., Liu, J., Christofides, P.D., 2012. Economic model predictive control of nonlinear process systems using Lyapunov techniques. AIChE J. 58 (3), 855–870. http://dx.doi.org/10.1002/aic.12672.

Hu, W., Hadler, K., Neethling, S.J., Cilliers, J.J., 2013. Determining flotation circuit layout using genetic algorithms with pulp and froth models. Chem. Eng. Sci. 102, 32–41. http://dx.doi.org/10.1016/j.ces.2013.07.045.

Huang, R., Harinath, E., Biegler, L.T., 2011. Lyapunov stability of economically oriented NMPC for cyclic processes. J. Process Control 21, 501–509. http://dx.doi.org/10.1016/j.jprocont.2011.01.012.

Jamett, N., Cisternas, L.A., Vielma, J.P., 2015. Solution strategies to the stochastic design of mineral flotation plants. Chem. Eng. Sci. 134, 850–860. http://dx.doi.org/10.1016/j.ces.2015.06.010.

Jämsä-Jounela, S.L., Dietrich, M., Halmevaara, K., Tiili, O., 2003. Control of pulp levels in flotation cells. Control Eng. Pract. 11 (1), 73–81. http://dx.doi.org/10.1016/S0967-0661(02)00142-9.

Liang, Y., He, D., Su, X., Wang, F., 2020. Fuzzy distributional robust optimization for flotation circuit configurations based on uncertainty theories. Miner. Eng. 156, http://dx.doi.org/10.1016/j.mineng.2020.106433.

Liu, X., Cui, J., 2018. Economic model predictive control of boiler-turbine system. J. Process Control 66, 59–67. http://dx.doi.org/10.1016/j.jprocont.2018.02.010.

Liu, J., MacGregor, J., Duchesne, C., Bartolacci, G., 2005. Flotation froth monitoring using multiresolutional multivariate image analysis. Miner. Eng. 18 (1), 65–76. http://dx.doi.org/10.1016/J.MINENG.2004.05.010.

Liu, S., Zhang, J., Liu, J., 2015. Economic MPC with terminal cost and application to oilsand separation. IFAC-PapersOnLine 28 (8), 20–25. http://dx.doi.org/10.1016/j.ifacol.2015.08.151.

Mahmoodi, S., Poshtan, J., Jahed-Motlagh, M.R., Montazeri, A., 2009. Nonlinear model predictive control of a pH neutralization process based on Wiener-Laguerre model. Chem. Eng. J. 146 (3), 328–337. http://dx.doi.org/10.1016/j.cej.2008.06.010.

Maldonado, M., Desbiens, A., Del Villar, R., 2009. Potential use of model predictive control for optimizing the column flotation process. Int. J. Miner. Process. 93, 26–33. http://dx.doi.org/10.1016/j.minpro.2009.05.004.

Maldonado, M., Desbiens, A., Del Villar, R., Quispe, R., 2007. Towards the optimization of flotation columns using predictive control. IFAC Proc. Vol. (IFAC-PapersOnline) 12 (PART 1), 75–80. http://dx.doi.org/10.3182/20070821-3-CA-2919.00011.

Mesa, D., Quintanilla, P., Reyes, F., 2022. Bubble Analyser - An open-source software for bubble size measurement using image analysis. Miner. Eng. 180, http://dx.doi.org/10.1016/j.mineng.2022.107497.

Navia, D., Puen, A., Quintanilla, P., Bergh, L., Briceño, L., de Prada, C., 2018. A proposal to include the information of disturbances in modifier adaptation methodology for real time optimization. Comput. Aided Chem. Eng. 43, 1081–1086. http://dx.doi.org/10.1016/B978-0-444-64235-6.50189-3.

Navia, D., Puen, A., Quintanilla, P., Briceño, L., Bergh, L., 2019. On dealing with measured disturbances in the modifier adaptation method for real-time optimization. Comput. Chem. Eng. 128, 141–163. http://dx.doi.org/10.1016/j.compchemeng.2019.06.004.

Neethling, S.J., Brito-Parada, P.R., 2018. Predicting flotation behaviour - The interaction between froth stability and performance. Miner. Eng. 120 (December 2017), 60–65. http://dx.doi.org/10.1016/j.mineng.2018.02.002.

Pérez-García, E.M., Bouchard, J., Poulin, 2021. Integrating online mineral liberation data into process control and optimisation systems for grinding - separation plants. J. Process Control 105, 169–178. http://dx.doi.org/10.1016/j.jprocont.2021.07.014.

Qin, S.J., Badgwell, T.A., 1997. An overview of industrial model predictive control technology. In: AIche symposium series. 93, (316), New York, NY: American Institute of Chemical Engineers, 1971-c2002., pp. 232–256.

Quintanilla, P., Navia, D., Moreno, F., Neethling, S.J., Brito-Parada, P.R., 2023. A methodology to implement a closed-loop feedback-feedforward level control in a laboratory-scale flotation bank using peristaltic pumps. MethodsX 10, http://dx.doi.org/10.1016/j.mex.2023.102081.

Quintanilla, P., Neethling, S.J., Brito-Parada, P.R., 2021a. Modelling for froth flotation control: A review. Miner. Eng. 162, 106718. http://dx.doi.org/10.1016/j.mineng.2020.106718.

Quintanilla, P., Neethling, S.J., Mesa, D., Navia, D., Brito-Parada, P.R., 2021b. A dynamic flotation model for predictive control incorporating froth physics. Part II: Model calibration and validation. Miner. Eng. 173 (November), 107190. http://dx.doi.org/10.1016/j.mineng.2021.107190.

Quintanilla, P., Neethling, S.J., Navia, D., Brito-Parada, P.R., 2021c. A dynamic flotation model for predictive control incorporating froth physics. Part I: Model development. Miner. Eng. 173 (November), 107192. http://dx.doi.org/10.1016/j.mineng.2021.107192.

Rawlings, J.B., Angeli, D., Bates, C.N., 2013. Fundamentals of economic model predictive control. In: Proceedings of the IEEE Conference on Decision and Control. pp. 3851–3861. http://dx.doi.org/10.1109/CDC.2012.6425822.

Riquelme, A., Desbiens, A., Del Villar, R., Maldonado, M., 2015. Identification of a non-linear dynamic model of the bubble size distribution in a pilot flotation column. Int. J. Miner. Process. 145, 7–16. http://dx.doi.org/10.1016/J.MINPRO.2015.11.003.

Riquelme, A., Desbiens, A., Del Villar, R., Maldonado, M., 2016. Predictive control of the bubble size distribution in a two-phase pilot flotation column. Miner. Eng. 89, 71–76. http://dx.doi.org/10.1016/j.mineng.2016.01.014.

Rohman, F.S., Aziz, N., 2019. Comparison of orthogonal collocation, control vector parameterization and multiple shooting for optimization of acid recovery in batch electrodialysis. AIP Conf. Proc. 2124, http://dx.doi.org/10.1063/1.5117073.

Sbarbaro, D., del Villar, R., 2010. Advanced Control and Supervision for Mineral Processing. Advances in Industrial Control, http://dx.doi.org/10.1007/978-1-84996-106-6.

Sbarbaro, D.G., Maldonado, M., Cipriano, A., 2008. A two level hierarchical control structure for optimizing a rougher flotation circui. In: IFAC Proceedings Volumes (IFAC-PapersOnline). http://dx.doi.org/10.3182/20080706-5-KR-1001.2619.

Schäfer, P., Caspari, A., Mhamdi, A., Mitsos, A., 2019. Economic nonlinear model predictive control using hybrid mechanistic data-driven models for optimal operation in real-time electricity markets: In-silico application to air separation processes. J. Process Control 84, 171–181. http://dx.doi.org/10.1002/aic.16568.

Schena, G., Villeneuve, J., Noël, Y., 1996. A method for a financially efficient design of cell-based flotation circuits. Int. J. Miner. Process. 46 (1–2), 1–20. http://dx.doi.org/10.1016/0301-7516(95)00082-8.

Serban, R., Petra, C., Hindmarsh, A.C., Balos, C.J., Gardner, D.J., Reynolds, D.R., Woodward, C.S., 2021. User Documentation for idas v4.7.0 (sundials v5.7.0). Technical Report.

Shean, B., Hadler, K., Cilliers, J.J., 2017. A flotation control system to optimise performance using peak air recovery. Chem. Eng. Res. Des. 117, 57–65. http://dx.doi.org/10.1016/j.cherd.2016.10.021.

Shean, B., Hadler, K., Neethling, S., Cilliers, J.J., 2018. A dynamic model for level prediction in aerated tanks. Miner. Eng. 125, 140–149. http://dx.doi.org/10.1016/j.mineng.2018.05.030.

Tsang, T.H., Himmelblae, D.M., Edgar, T.F., 1975. Optimal control via collocation and nonlinear programming. Internat. J. Control 21 (5), 763–768. http://dx.doi.org/10.1080/00207177508922030.